SCOPE | SAUDI INTERNATIONAL CONFERENCE ON NUCLEAR POWER ENGINEERING

Proceedings of SCOPE
13-15 Nov. 2023 – KFUPM
Paper 23096

An Efficient Approach for Benchmarking Axial Flow-Induced Vibration for Nuclear Applications

Anas Muhamad Pauzi[1, 2 a)], Hector Iacovides[1] and Andrea Cioncolini[3]
[1]*Department of Mechanical, Aerospace & Civil Engineering, University of Manchester, United Kingdom*
[2]*College of Engineering, Universiti Tenaga Nasional (UNITEN), Malaysia*
[3]*Guangdong Technion-Israel Institute of Technology [GTIIT], Shantou, Guangdong, China*
Corresponding Email: anas@uniten.edu.my/ anasmpauzi@gmail.com

Abstract – *Fretting wear at the spacer grid in fuel assemblies, due to flow-induced vibration (FIV), is one of the main causes of fuel failures in Light Water Reactors (LWRs). Therefore, accurately predicting FIV is crucial for mitigating this issue, and a computationally efficient simulation method is necessary. In this regard, the Unsteady Reynolds-Averaged Navier-Stokes (URANS) approach is applied as a promising and efficient simulation method for FIV prediction. While previous studies have primarily relied on Large Eddy Simulation (LES) for the fluid domain, URANS provides an attractive alternative due to its lower computational demands, especially for strong 2-way Fluid-Structure Interaction (FSI) coupling. This paper aims to explore efficient approaches for benchmarking axial FIV for nuclear applications by examining the self-exciting axial FIV over a cantilevered rod and comparing it with experimental measurements at the University of Manchester (UoM) using different URANS models and divergence schemes for the convection term in the fluid momentum equations. In both variations of the URANS model closure, the eddy viscosity model (EVM) k-**ω** SST model and the Reynolds Stresses Model (RSM) Launder, Reece, and Rodi (LRR) model, accurately predicted the mean RMS amplitude and frequency of vibration.*

Keywords: Flow-Induced Vibration (FIV), Fluid-Structure Interaction (FSI), Nuclear Fuel

I. Introduction

Flow-induced vibration (FIV) arises in nuclear fuel rods because of their loosely assembled fuel rods with springs at both ends and spacer grids that accommodate thermal expansion during operation. Predicting FIV requires robust 2-way Fluid-Structure Interaction (FSI) simulations that accurately model turbulence in fluid flow and the precise mechanical response of the rods, but this requires considerable computational resources. Hence, this paper suggests an efficient approach to achieve accurate predictions in line with the desired objectives.

In relation to FIV and fretting wear, four primary objectives are typically studied in nuclear applications. The first is flow field measurement, which has also been widely examined in the context of heat transfer and turbulent mixing with variations in grid assembly and fuel assembly design **[1]**. The second is vibration modes, which must be identified to prevent the rod from vibrating at its natural frequencies. The third is vibration damping upon displacement, exemplified by varying tailing end cap shapes **[2]**. It is desirable that the rod and flow channel designs provide as much damping as possible to minimise fretting wear at the grid assembly, especially during reactor start-up, shutdowns, and in accident scenarios. Finally, the fourth objective is determining the mean RMS amplitude of vibration, to identify the maximum flow velocity before the rod reaches dynamic instabilities such as flutters and static divergence **[3]**, which would accelerate fuel failures.

Different optimisation levels are needed for each objective. For example, predicting the modes and mean RMS amplitude of vibration using a semi-empirical model requires the input of an accurate flow field from high-fidelity flow models **[1]**. In contrast, predicting damping in axial turbulent flow can be achieved with laminar flow models that simulate average flow without accounting for turbulence **[4]**. Lastly, when predicting the mean RMS amplitude of vibration from self-excited FIV, it is important to reproduce the unsteady flow behaviour

of turbulent flow in order to simulate the mechanical vibration response, without the need for a high-fidelity flow model **[5]**.

II. Literature Review

Experiments at the University of Manchester investigated axial water flow on a cantilever rod in an annular flow channel, including flow field measurements near the free end and corresponding mechanical responses **[3]**.

Two simulation studies have been performed: firstly, by De Santis and Shams in 2019, using a combined finite volume method for the fluid domain and finite element method for the solid domain (FVM-FEM) approach **[4]**; and secondly, by Salachna et al. in 2023 using the FVM-FVM approach **[5]**. Both studies achieved good accuracy with the frequency of vibration when the fluid flow was resolved using the URANS Eddy Viscosity Model (EVM) k-ω SST model **[6]**, but were unable to obtain self-induced FIV **[4]** and achieved a mean RMS amplitude of vibration three orders of magnitude lower than the experimental measurements. The reason for this discrepancy was identified as the inability of the EVM URANS model to reproduce the flow's unsteady behaviour near the rod's free end. Both previous studies managed to address this by including an artificial random number generator to model the turbulent pressure field, known as the Pressure Fluctuating Model (PFM) **[3]**, and also by using the Reynolds Stresses Model (RSM) Launder, Reece, and Rodi (LRR) **[7]**.

III. Methodologies

III.A. Mathematical Models

The fluid and solid domains are solved separately and coupled using a robust two-way FSI algorithm. Firstly, the governing equation for solid deformation is derived from the force-equilibrium equation using the Hookean linear elastic equation and small strain assumption. It is then rearranged to be solved with explicit treatment in the linear solver to enhance stability **[8]**. The solid displacement equation is given as follows.

$$\rho_s \frac{\partial^2 u_i}{\partial t^2} - \underbrace{[2\mu+\lambda]\frac{\partial}{\partial x_i}\left(\frac{\partial u_j}{\partial x_j}\right)}_{implicit} - \underbrace{\frac{\partial}{\partial x_i}\left(\mu\frac{\partial u_i}{\partial x_j} + \lambda\delta_{ij}\frac{\partial u_i}{\partial x_i} + [\mu+\lambda]\frac{\partial u_j}{\partial x_j}\right)}_{explicit} = -\rho_s f_i \quad (1)$$

u is the solid deformation, ρ_s is the density of the solid, μ and λ are the Lame's constant which represents the elasticity, and f is the body force.

Next, the fluid flow is derived from the mass and momentum balance and modified for a moving mesh using the Arbitrary Lagrangian-Eulerian (ALE) Formulation. The Navier-Stokes equations with ALE formulation are given as follows.

$$\frac{\partial U_i}{\partial t} + \frac{\partial}{\partial x_j}(U_i - w_i)U_j = -\frac{1}{\rho_f}\frac{\partial P}{\partial x_i} + \nu\frac{\partial}{\partial x_j}\left(\frac{\partial U_i}{\partial x_j}\right) + F_i \quad (2)$$

U, P, ρ_f, and F are the flow velocity, pressure, density, and body force, while w is the velocity of the moving mesh, solved using the Laplace equation as follows.

$$\frac{\partial}{\partial x_i}\left(\gamma\frac{\partial w_i}{\partial x_j}\right) = 0 \quad (3)$$

γ is the diffusion coefficient which governs the distribution of fluid mesh upon motion at the FSI interface, given as the quadratic of the inverse distance for optimised preservation of mesh quality during fluid mesh deformation **[9]**.

Furthermore, in the fluid flow, which involves high Reynolds numbers, the turbulent eddies are modelled as Reynolds stresses and have been tested with both closures, EVM and RSM. The EVM model uses the Boussinesq hypothesis to assume the Reynolds stresses, R, as follows.

$$R_{ij} = -\rho_f\overline{u_i u_j} = \mu_t\left(\frac{\partial U_i}{\partial x_j} + \frac{\partial U_j}{\partial x_i}\right) - \frac{2}{3}\left(\rho_f k + \frac{\mu_t}{2}\frac{\partial U_k}{\partial x_k}\right)\delta_{ij} \quad (4)$$

k and μ_t are the turbulent kinetic energy and the turbulent viscosity respectively, and solved using the k-ω SST model **[6]** using transport equations. The RSM model on the other hand solves the six components of the Reynolds Stresses by solving the transport of kinematic Reynolds stresses as follows

$$\frac{\mathrm{D}R_{ij}}{\mathrm{D}} = P_{ij} - \epsilon_{ij} + \phi_{ij} - D_{ij} \quad (5)$$

P, ε, ϕ and D are the production, dissipation, pressure-strain, and diffusion terms respectively and solved using the LRR model using six equations **[7]**. Furthermore, a high Reynolds number wall function is used to model the near-wall flow profile, thereby improving mesh quality and enhancing computational efficiency without requiring a fine mesh near the wall to fully resolve the flow.

Finally, the FSI interface is connected using the kinetic and dynamic boundary conditions given as follows respectively.

$$u_{F,i} = u_{S,i} \tag{6}$$

$$t_{F,i} = n_i \sigma_{S,i} \tag{7}$$

u_F and u_S are the displacement of the vertices for the fluid and solid mesh, while t_F and σ_S are the fluid traction force and solid stress at the FSI interface.

III.B. Numerical Solutions

Both the fluid and solid domains are discretized using the FVM. The solid domain is discretized spatially and temporally using second-order schemes. Spatially, the implicit term is solved using the central difference scheme with skewness and non-orthogonal correction, while the explicit terms are solved using the weighted least-squares approach. Temporal terms for both solid and fluid domains are discretized using the implicit second-order Euler method.

Meanwhile, in the fluid domain, the divergence schemes for the momentum equations are discretized using the central difference schemes to enhance unsteady behaviour in the flow. The divergence schemes for the transport equations for the turbulent variables are solved using the first-order upwind scheme to ensure the stability of the simulation.

The FSI coupling is solved using the IQN-ILS algorithm **[10]**, and the simulations are performed using Foam-Extend-4.0 with the Solids4Foam extension **[11]**.

III.C. Experiment Setup

In the UoM experiment, axial flow with a Reynolds number ranging from 16,400 to 90,000 flows vertically in a tube channel towards a cantilevered rod, causing the rod to self-excite and vibrate. At a Reynolds number of around 70,000, the rod's vibration begins to experience instability, exhibiting flutter-like motion and alternating between large amplitude deflection and small-amplitude random vibration. Due to the use of the ALE formulation for the moving fluid mesh, simulations were conducted within the small-amplitude region to avoid errors arising from mesh skewness and non-orthogonality during large deformation in the narrow annulus gap.

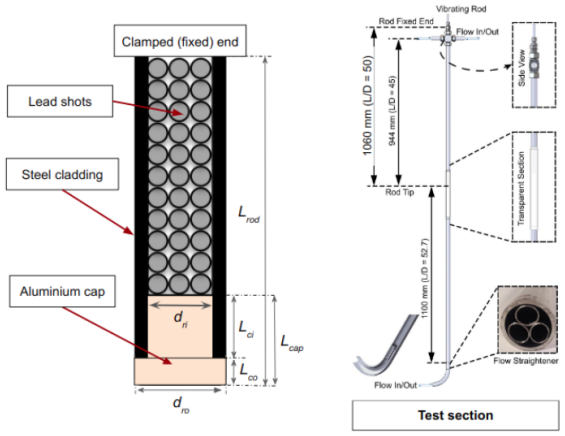

*Fig. 1. Schematic of the cantilevered rod in the UoM experiment and the test piece section (right) **[3]**.*

The schematic of the UoM axial FIV experiment is given in Fig. 1, while the corresponding geometrical and material properties used for the simulation are given in Table 1.

Table I. Properties of the UoM cantilever rod single material models and the flow channel.

Variables	Values
Solid domain	
Length of rod, L [mm]	1060
Rod outer diameter, d_{ro} [mm]	10.01
Rod inner diameter, d_{ri} [mm]	8.83
Rod cap length, L_{cap} [mm]	1.32
Rod linear mass density, m [kg/m]	0.588
Density of solid, ρ_S [kg/m^3]	33676.3
Young's modulus, E [GPa]	202.26
Second moment of inertia,, I [mm^4]	194.4
Number of solid mesh	65k - 90k
Fluid domain	
Tube channel diameter, d_{ti} [mm]	21.0
Length of inlet region, L_{in} [mm]	63
Density of fluid, ρ_f [kg/m^3]	997.84
Dynamic viscosity of fluid, μ [kg/m.s]	9.659 x10^{-4}
Linear added mass, m_{add} [kg/m]	0.124
Annulus Reynolds number, Re_{ann}	16,400-61,730
Number of fluid mesh	600k - 750k

As illustrated in Fig. 1, the experimental cantilevered rod comprises a steel tube filled with variable-sized lead shot and capped with aluminium. To improve efficiency and simplify the simulation, the rod was modelled as a single material using the Beam-Bernoulli equation, which was used to predict the modes of vibration (f). The equation is given as follows:

$$f_i = \frac{\beta_i^2}{2\pi}\sqrt{\frac{EI}{(\dot{m}_{rod} + \dot{m}_{add})\,L^4}} \tag{8}$$

β is the influence factor, given by 1.875 for the first mode of vibration of a cantilever, f_1 is the first mode of vibration in still water, measured in the experiment as 3.71Hz **[3]**, while all other parameters are given in Table 1. This assumption had proved good accuracy in simulation involving vibration in still water and also in axial FIV **[12]**.

IV. Results and Discussions

Prior to performing the two-way FSI simulation, the fluid domain is validated against PIV measurement **[13]**, for the annulus Reynolds number 35,100, representing the middle of the range.

The velocity profile at $0.45d_{ti}$ downstream of the free rod in Fig. 2 shows that the both URANS models result in relatively similar velocity profiles, axially and radially. However, the LRR model proves to be more accurate than the k-ω SST model, hence, initial validation was performed using the LRR model.

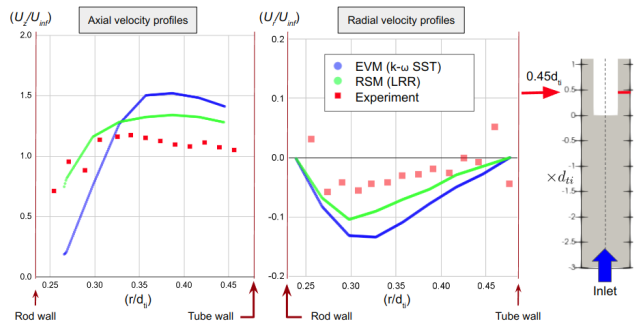

*Fig. 2. The axial velocity profile at ($0.45d_{ti}$) downstream of the free end for the experiment's PIV data **[13]** and the simulations with different URANS models.*

Initially, simulations for both URANS models were conducted using a 1st order upwind scheme for the momentum equations to stabilise the simulation. However, the velocity time series displayed steady state behaviour. After switching to a 2nd order central difference scheme, unsteady flow emerged and persisted throughout the simulation downstream of the rod's free end in both URANS models, as depicted in Fig.3. Both models exhibited similar velocity fluctuations, approximately 1 m/s in range, but the k-ω SST model showed a marginally higher average velocity, both downstream near the free end and in the maximum velocity within the fluid domain.

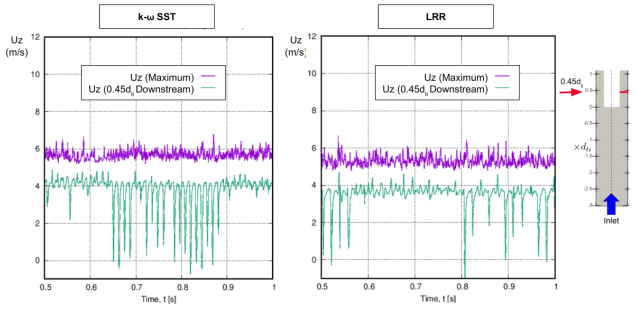

Fig. 3. Axial flow velocity time series at ($0.45d_{ti}$) downstream location and the maximum velocity for the k-ω SST model (left) and the LRR model (right).

Using the validated fluid domain, self-excite FIV simulation is performed in stages, firstly with 1-way, and then a 2-way FSI coupling to ensure stability throughout the simulation.

The bottleneck in the computation primarily occurs due to the solid solver. Therefore, optimisation could be achieved by limiting the number of iterations for the solid inter-component coupling solver (nCorr). This has been proven to maintain the frequency of vibration while gradually increasing the numerical damping in the study of free vibration in the solid-only domain **[5, 12]**. Further comparisons are performed by varying the limit on the number of iterations for the axial FIV simulation against the mean RMS amplitude and first mode of vibration for the axial FIV.

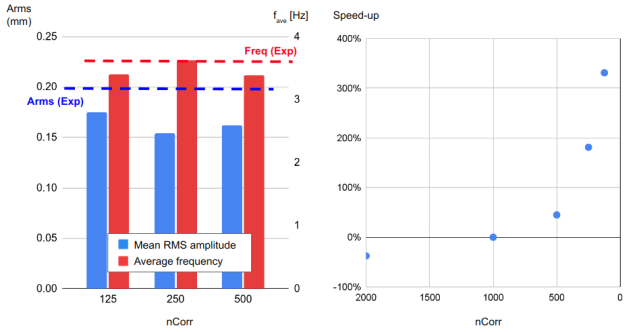

Fig. 4. Comparing the limit number of solid correctors iteration (nCorr) with the resultant RSM amplitude and the first mode of vibration (left) and the computation speed-up compared to the 1000 corrector iteration limit.

Fig. 4 shows that reducing the limit number of iteration for the solid solver would cause significant changes in both RMS amplitude and frequency of vibration, but the computational time reduces exponentially.

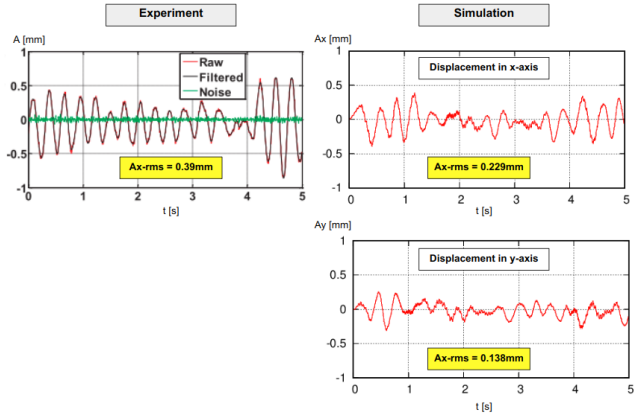

*Fig. 5. Displacement time series for a 5-second simulation; comparing the simulation in the experiment (right)**[13]** and the x- and y-directions (top left and bottom left respectively).*

The comparison of the displacement time series in Fig. 5 reveals similar small-amplitude random vibrations in both the simulation and experiment. Despite the experimental mean RMS amplitude being obtained for a 300 seconds sample, the 5-second displacement time series in Figure 5 has an almost doubled mean RMS amplitude. This suggests a range of uncertainties and supports the adequacy of the 5-second simulation data in representing the mean RMS amplitude.

The modes of vibration were obtained by performing the Fast Fourier Transformation (FFT) analysis on the time-displacement series.

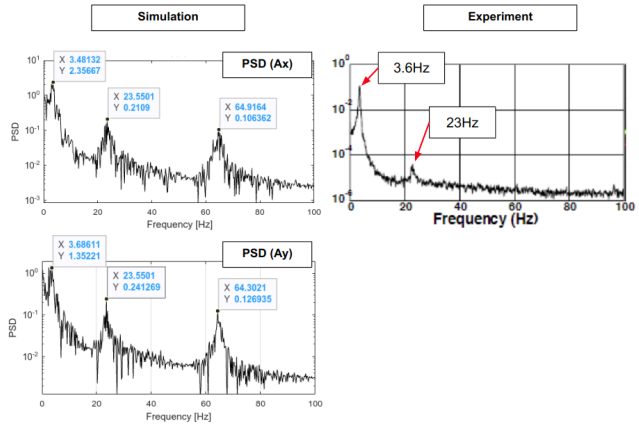

*Fig. 6. Power spectral density (PSD) of displacement time series from simulation in the x- and y-axis (top and bottom left respectively) and from experiment **[13]**.*

Fig. 6 shows that the simulation reveals good accuracy for both the 1st and 2nd modes of vibration and also reveals the 3rd mode of vibration, which could not be seen in the experiment data. This discrepancy may have been caused by the application of moving averaging on the displacement time-series from the experiment, which filtered out higher frequency noises originating from distant sources, such as pump vibrations. This demonstrates the simulation's potential for future analyses involving modes of vibration, to analyse the internal structures of the rod.

Simulations were repeated for the k-ω SST model and for a range of Reynolds number from 16,400 to 61,730 with slight adjustment on the mesh to adhere to the recommended near-wall node distance of applying the high Reynolds number wall functions.

Fig. 7 and Fig. 8 show good agreement with the experimental data for both URANS models, which is within the uncertainty of the experimental data. Both URANS models exhibit similar trends of increasing mean RMS amplitude and a slight decrease in the 1st mode of vibration from the value of the first mode of vibration in still water, 3.71Hz, as the Reynolds number increases.

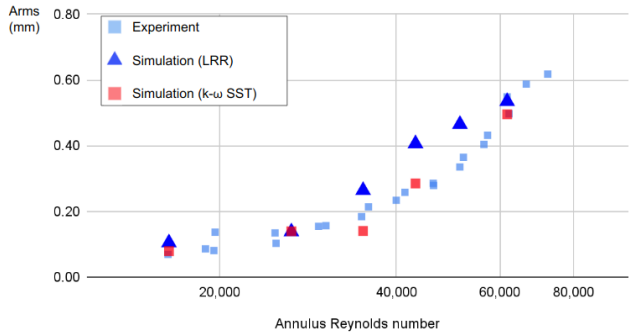

Fig. 7. Mean RMS amplitude of vibration at varying Reynolds numbers.

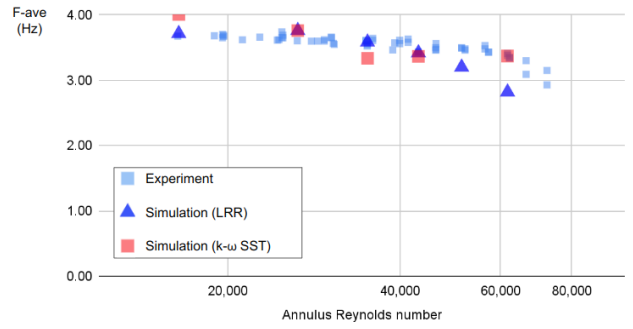

Fig. 8. The first mode vibration at varying Reynolds numbers

Simulations at higher Reynolds numbers faced challenges in maintaining stability and occasionally

experienced divergence due to high fluctuations in flow variables. An error occurred when restarting the simulation, which was associated with the high lift coefficient observed during the first few iterations upon restarting. Compared to the LRR model, the k-ω SST model proved to be less stable and required more computational resources.

IV. Conclusions

This research focused on axial flow-induced vibration (FIV) within the nuclear industry, a significant contributor to fretting wear in nuclear fuel rods. The study used numerical simulations to predict FIV and validated them against experiments conducted at the University of Manchester.

The University of Manchester's experiment, which employed a cantilevered rod setup, was found to be advantageous due to its ability to reproduce flow instabilities and facilitate the prediction of the mean RMS amplitude of vibration.

Flow instabilities were reproduced using a variety of URANS closure models. Despite challenges at higher Reynolds numbers, the simulation remained reasonably accurate. However, limitations became evident at these higher Reynolds numbers, with divergences occurring due to significant velocity fluctuations in the flow domain.

Comparing both URANS models, the LRR exhibited better accuracy in the flow domain and superior stability during axial FIV, as compared to the k-ω SST model.

This simulation methodology could be useful in predicting the FIV phenomenon across a wider range of applications involving high-stiffness materials in axial turbulent flow, especially in flow domains experiencing large flow instabilities, such as those with helically wrapped wire around the rod. For future work involving higher Reynolds numbers to predict critical velocities for vibration instabilities, such as flutter and static divergence, changes in the moving mesh formulation will be required to prevent issues arising from diminishing mesh quality due to excessive deformation.

Acknowledgements

This publication is part of the postgraduate study sponsored by the Malaysian government via Majlis Amanah Rakyat (MARA) and supported by the National Energy University (UNITEN), Malaysia.

References

1. Conner, M.E., Baglietto, E. and Elmahdi, A.M. (2010) ‘CFD methodology and validation for single-phase flow in PWR fuel assemblies’, Nuclear Engineering and Design, 240(9), pp. 2088–2095.
2. Wambsganss, M.W. and Jendrzejczyk, J.A. (1979) ‘The effect of trailing end geometry on the vibration of a circular cantilevered rod in nominally axial flow’, Journal of Sound and Vibration, 65(2), pp. 251–258.
3. Cioncolini, A., Zhang, S., Nabawy, M. R. A., Li, H., Cooper, D., & Iacovides, H. (2023). Annals of Nuclear Energy Experiments on axial-flow-induced vibration of a free-clamped / clamped-free rod for light-water nuclear reactor applications. Annals of Nuclear Energy, 190(January), 109900
4. De Santis, D., & Shams, A. (2019). An advanced numerical framework for the simulation of flow-induced vibration for nuclear applications. Annals of Nuclear Energy, 130, 218–231
5. Salachna, J., Cioncolini, A. and Iacovides, H. (2023) ‘Benchmark simulation of the flow-induced vibrations for nuclear applications’, Annals of Nuclear Energy, 180(July 2022), p. 109425.
6. Menter, F. R. (1994). Two-equation eddy-viscosity turbulence models for engineering applications. AIAA Journal, 32(8), 1598–1605.
7. Launder, B. E., Reece, G. J., & Rodi, W. (1975). Progress in the development of a Reynolds-stress turbulence closure. Journal of Fluid Mechanics, 68(3), 537–566.
8. Jasak, H. and Weller, H.G. (2000) ‘Application of the finite volume method and unstructured meshes to linear elasticity’, International Journal for Numerical Methods in Engineering, 48(2), pp. 267–287
9. Jasak, H., & Tuković, Ž. (2006). Automatic mesh motion for the unstructured Finite Volume Method. Transactions of Famena, 30(2), 1–20.
10. Degroote, J., Bathe, K. J., & Vierendeels, J. (2009). Performance of a new partitioned procedure versus a monolithic procedure in fluid-structure interaction. Computers and Structures, 87(11–12), 793–801.
11. Cardiff, P., Karač, A., De Jaeger, P., Jasak, H., Nagy, J., Ivanković, A., & Tuković, Ž. (2018). An open-source finite volume toolbox for solid mechanics and fluid-solid interaction simulations.
12. Muhamad Pauzi, A., Iacovides, H. and Cioncolini, A. (2023) ‘Pragmatic modelling of axial flow-induced vibration (FIV) for nuclear fuel rods’, in IOP Conf. Series: Materials Science and Engineering. Bangi, Malaysia: IOP Publishing.
13. Cioncolini, A., Silva-Leon, J., Cooper, D., Quinn, M. K., & Iacovides, H. (2018). Axial-flow-induced vibration experiments on cantilevered rods for nuclear reactor applications. Nuclear Engineering and Design, 338(August), 102–118